$k = 0$ Libron Spectrum for Solid Hydrogen in the $Pa3$ and C_{mmm} Structures*

Cornelius F. Coll, III, and A. Brooks Harris
Department of Physics, University of Pennsylvania, Philadelphia, Pennsylvania 19104
(Received 27 March 1970)

The libron wave spectrum at zero wave vector for solid hydrogen in the $Pa3$ and C_{mmm} structures is calculated at zero temperature. Interactions other than the electrostatic interactions between molecular quadrupole moments are treated perturbatively. Comparison of our numerical and analytic results for libron frequencies and Raman intensities with the observed Raman spectrum gives strong evidence for the $Pa3$ structure. The scaling relation between the frequencies of the classical and quantum-librational systems is found to hold for the $Pa3$ but not for the C_{mmm} structure. The effects of zero-point librations and libron-libron interactions are studied to lowest order in $1/z$, where z is the number of nearest neighbors. Although the static effects are quite small, the shifts in the libron frequencies due to these interactions are of order 15%.

I. INTRODUCTION

The problem of understanding the cooperative nature of the orientational state of solid hydrogen[1] has been the object of a number of studies, both experimental and theoretical. In spite of this work, although many aspects of the ordering of the molecular axes are now well understood, others remain unexplained. For instance, it is quite clear that the elementary excitations are libron waves,[2-7] and yet the details of the crystal structure of the ordered state, e.g., the size of the "magnetic" unit cell, remain unclear. In this regard, thermodynamic measurements are not very informative because the bulk properties of solid hydrogen do not depend sensitively on the precise way in which the ordering of molecular axes takes place. To resolve this structural ambiguity, resonant measurements such as optical experiments or neutron or x-ray spectroscopy are more helpful.

For instance, Hardy *et al.*[7] have shown that the undistorted $Pa3$ structure is not entirely consistent with the Raman spectrum of solid H_2 and D_2 at nearly 100% concentration of $(J=1)$ molecules. Nor were they able to find a distortion[8] which would explain all their data. More recently, James has suggested[9] that there may be a temperature range just below the ordering temperature where a different structure is thermodynamically stable. According to Hardy,[10] the symmetry of space group C_{mmm} (see note added in proof in Ref. 27) proposed by James is consistent with the optically observed $(J=0)-(J=2)$ rotational excitations. Accordingly, it seemed important to calculated the libron spectrum and associated Raman intensities for this structure. If, as is usual, one assumes that the electrostatic quadrupole-quadrupole (EQQ) interactions dominate the orientational interactions, then the resulting libron modes do not at all agree with the observed Raman spectrum. Allowing for the possibility of more general interactions does enable one to fit the frequencies of the Raman spectrum, although even then, the intensities do not reproduce the observed spectrum very well. Thus, in order to explain the Raman spectrum it is necessary to postulate (i) very-large non-EQQ interactions and (ii) structural distortions sufficiently large as to alter considerably the intensity ratios. Since these possibilities, when taken together, seem improbable, and since the neutron-diffraction data[11] are consistent with the $Pa3$ structure, we conclude that the C_{mmm} structure is not actually realized.

We should also point out that lately other indications have become apparent which disfavor the C_{mmm} structure. For instance, James's original proposal was based on considering nearest-neighbor interactions only. More recently, however, he finds[12] that inclusion of further-neighbor interactions renders the C_{mmm} structure thermodynamically unstable relative to the $Pa3$ structure. This tendency is also apparent from our libron-wave calculations. Second, more detailed calculations of Hardy *et al.*[13] show that although the symmetry of the C_{mmm} structure is consistent with the observed four-line spectrum corresponding to the $(J=0)-(J=2)$ transitions, the actual absorption spectrum does not agree qualitatively with theory. On the basis of these two calculations, together with those presented here, it is quite clear that the structure of solid hydrogen is not of the type C_{mmm}.

A secondary objective of this paper was to formulate the problem of libron-libron interactions in a systematic way. This can be done in close analogy with the problem of interactions between spin waves in an antiferromagnet.[14,15] Although the results of the various calculations[2,3,4,16] of zero-point effects on the thermodynamic properties do not agree with one another exactly, they do indicate that these effects are small. One might expect, similarly, the effect of zero-point motion on the excitation spectrum to be small. We have studied

these effects using the $1/z$ expansion and find surprisingly large, e.g., of order 15%, dynamical corrections to the average libron energy due to zero-point motion. In view of these results, we are pursuing more detailed calculations to obtain the energy shifts of the individual libron energies due to zero-point effects. Furthermore, the presence of strong libron-libron interactions undoubtedly plays a crucial role in the broadening observed in the highest-energy libron mode.[7]

Briefly, this paper is organized as follows. In Sec. II, we study the equations of motion for noninteracting librons. We show that the dynamical matrix can be reduced to dimensionality $2s$ under rather general assumptions about the lattice structure, where s is the number of sublattices. Our results for the $Pa3$ structure agree with those of previous authors.[2-5] In Sec. III, we derive formulas for the intensities of the Raman scattering spectrum, based on the polarizability approximation.[17] In Sec. IV, we investigate the effect of zero-point motion on both the thermodynamic properties and the libron energy gap. The effect on the thermodynamic properties is small. In contrast, the effect on the libron energy spectrum is quite significant. In Sec. V, we discuss our numerical and analytic results for the libron frequencies and Raman intensities for both the C_{mmm} and $Pa3$ structures. As mentioned above, our results strongly favor the $Pa3$ structure. In Appendix A, we clarify the relationship between the libron spectrum of quantum and classical[18] systems. Although the frequencies are proportional for structures of high symmentry such as the $Pa3$, the relationship[19] is not the usual equivalence between the problem of small oscillations in the classical and quantum limits. Finally, the interaction coefficients γ_{ij}^{mn} defined in Eq. (9), below, are tabulated in Appendix B assuming nearest-neighbor EQQ interactions only.

II. HAMILTONIAN AND EQUATION OF MOTION FOR LIBRONS

A. Discussion of Model

In this section, we shall give a rather general discussion or the equation of motion for libron waves in solid hydrogen. Although it is usually supposed that the dominant interactions between molecules in the solid are those between the electric quadrupole moments of the molecules,[20] we shall consider the most general pairwise interactions consistent with the symmetry of the diatomic molecules and the lattice structure of the solid. Since the energy gap between successive rotational kinetic-energy levels dominates the orientational interactions in the solid, the rotational angular momentum J_i of the molecule at the lattice site R_i is a good quantum number, and at low temperatures $J_i = 0$ or $J_i = 1$ depending on the nuclear spin of the molecule. Accordingly, in the expansion of the static intermolecular potential in spherical harmonics $Y_L^M(\hat{\omega}_i)$, where Y_L^M is the spherical harmonic in the phase convention of Rose,[21] and $\hat{\omega}_i$ denotes the pair $(\theta_{ij}^i, \varphi_{ij}^i)$ of spherical coordinates of the orientation of the ith molecule relative to a quantization axis parallel to $\vec{R}_{ij}$, where we write $\vec{R}_{ij} \equiv \vec{R}_i - \vec{R}_j$, and it is only necessary to consider terms involving Y_2^M or Y_0^0. The latter appear in "single-molecule" terms which have been shown by Nakamura to vanish in a rigid cubic or hcp lattice.[20] Thus, without loss of generality, we may consider the interaction between molecules to be effectively of the form

$$\mathcal{H}_{ij} = 4\pi\epsilon(R_{ij}) \sum_M a_M Y_2^M(\hat{\omega}_i) Y_2^M(\hat{\omega}_j)^* \quad , \tag{1}$$

where the a_M are constants obeying the relation $a_M = a_{-M}^*$ and $\epsilon(R_{ij})$ is a function of the intermolecular separation. It is convenient to rewrite Eq. (1) in the form suggested by Van Kranendonk[22]:

$$\mathcal{H}_{ij} = \sum_{J=0,2,4} \sum_M \epsilon_J(R_{ij}) \alpha_J C(22J; M, -M) \times Y_2^M(\hat{\omega}_i) Y_2^{-M}(\hat{\omega}_j), \tag{2}$$

where $C(j_1 j_2 j_3; m_1, m_2)$ is a Clebsch-Gordan coefficient,[21] $\epsilon_J(R_{ij})$ measures the strength of the coupling into a resultant total angular momentum J, and the constants α_J are $\alpha_4 = (70)^{1/2}$, $\alpha_2 = (\frac{7}{2})^{1/2}$, and $\alpha_0 = (5)^{1/2}$.

Accurate theoretical predictions of the constants ϵ_2 and ϵ_0 have not been performed up to now, although a rough idea of their magnitude can be obtained from the work of Margneau[23] and deBoer.[24] Since there have been no experimental determinations of either ϵ_0 or ϵ_2 to confirm these estimates, we shall consider these parameters as being adjustable. As pointed out by Nakamura,[20] however, they are probably dominated by the EQQ interactions which contribute exclusively to $\epsilon_4(R)$. Neglecting other contributions to $\epsilon_4(R)$, we may write

$$\epsilon_4(R) = (\tfrac{5}{6}\xi_0\Gamma_0)(R_0/R)^5, \tag{3}$$

where R_0 is the nearest-neighbor distance and Γ_0 is the EQQ coupling constant

$$\Gamma_0 = (6e^2Q^2/25R_0^5), \tag{4}$$

where eQ is the molecular quadrupole moment. The values of Γ_0 given in Table I agree fairly well with the experimental determinations of Γ_0 as is discussed in Refs. 6 and 25. Of course, there are several many-body effects which modify the EQQ interactions when an isolated pair of molecules is placed in the solid. The principle effects are[25] (i) static phonon renormalization, (ii) dynamic phonon renormalization, and (iii) screening effects.

TABLE I. Values of the interaction coefficients.

Equation	Parameter	H_2	D_2
	Calculated		
(4)	Γ_0[a]	0.698 cm^{-1}	0.839 cm^{-1}
(4)	Γ_0[a]	1.005 °K	1.206 °K
(5)	ξ_{scr}[b]	0.96	0.95
(5)	ξ_{ph}[c]	0.75–0.80	~0.80
(5)	ξ_0	0.72–0.77	~0.76
(68d)	ξ_{rot}	0.814	0.814
(71)	ξ	~0.62	~0.63
	Deduced from the Raman spectrum		
(71)	ξ	0.69	0.76

[a]For a detailed discussion of the values of Γ_0, see Ref. 25

[b]See Ref. 25.

[c]This estimate is obtained by combining the dynamic phonon renormalization of Γ in Ref. 25 with the static renormalization in Ref. 26. The latter is itself the result of two types of effects, viz., short- and long-range correlations. For D_2 it is clear that long-range correlations are less important than for H_2.

These are taken into account by the renormalization factor ξ_0 in Eq. (3), and we may write

$$\xi_0 = \xi_{ph}\,\xi_{scr}, \tag{5}$$

where ξ_{ph} pertains to the phonon effects and ξ_{scr} to the screening corrections. The best theoretical values of[25,26] these constants are listed in Table I. Since the effects of libron-phonon interactions are perturbative and can be handled in a separate calculation, we shall neglect them and treat solid hydrogen as a rigid lattice.

B. Libron Hamiltonian

Let us write Eq. (2) in terms of a quantization axis arbitrarily fixed with respect to the crystal axes:

$$\mathcal{H}_{ij} = 4\pi \sum_J \sum_{mm'} \epsilon_J(R_{ij})\,\alpha_J\,[4\pi/(2J+1)]^{1/2} \times C(22J; m, m')\,Y_2^m(\Omega_i) \times Y_2^{m'}(\Omega_j)\,Y_J^{m+m'}(\Omega_{ij})^*. \tag{6}$$

Here Ω_i and Ω_{ij} specify, respectively, the orientation of the axis of the ith molecule and that of the intermolecular axis $\vec{R}_{ij}$, both relative to the arbitrarily fixed quantization axis.

Following Raich and Etters,[4] we transform to a coordinate system in which the z axis for each molecule lies along its equilibrium orientation. This direction coincides with the direction of lowest energy for the ith molecule in the classical ground state.[27] Thus, the state when all the molecules have $J_z = 0$ is analogous to the Néel state of antiferromagnets. We have

$$Y_2^m(\Omega_i) = \sum_{m'} D^{(2)}_{mm'}(\chi_i)^*\,Y_2^{m'}(\omega_i), \tag{7}$$

where $D^{(J)}_{mm'}(\chi_i)$ is a rotation matrix,[21] where $\chi_i \equiv (\alpha_i, \beta_i, \gamma_i)$ is the triad of Euler angles[21] specifying the orientation of the local equilibrium axes with respect to the arbitrarily fixed quantization axes introduced in Eq. (6), and $\omega_i \equiv (\theta_i, \varphi_i)$ describes the orientation of the ith molecule relative to its local equilibrium axes. With these substitutions the Hamiltonian can now be written in terms of spherical harmonics referred to the local axes as

$$\mathcal{H} = \sum_{ij} \sum_{mm'} \gamma_{ij}^{mm'} O_i^m O_j^{m'}, \tag{8}$$

where

$$\gamma_{ij}^{mm'} = 4\pi A_m A_{m'} \sum_J \epsilon_J(R_{ij})\,\alpha_J\,[\pi/(2J+1)]^{1/2} \times \sum_{nn'} C(22J; n, n')\,D^{(2)}_{nm}(\chi_i)^* \times D^{(2)}_{n'm'}(\chi_j)^*\,Y_J^{n+n'}(\Omega_{ij})^*, \tag{9}$$

and following the notation of Raich and Etters[4]:

$$A_0 = -\tfrac{1}{10}(5/\pi)^{1/2}, \tag{10a}$$

$$A_{\pm 1} = \pm\tfrac{1}{20}(30/\pi)^{1/2}, \tag{10b}$$

$$A_{\pm 2} = -\tfrac{1}{20}(30/\pi)^{1/2}, \tag{10c}$$

and

$$O_i^0 = -\tfrac{5}{2}(3\cos^2\theta_i - 1), \tag{11a}$$

$$O_i^{\pm 1} = -5\cos\theta_i \sin\theta_i\, e^{\pm i\varphi_i}, \tag{11b}$$

$$O_i^{\pm 2} = -(\tfrac{5}{2})\sin^2\theta_i\, e^{\pm 2i\varphi_i}. \tag{11c}$$

The present discussion can be applied to any system of diatomic molecules governed by a Hamiltonian of the form Eq. (2). In particular, for molecules other than hydrogen one has $B \ll \hbar\omega_0$, where $\hbar\omega_0$ is a typical libron energy and B is the rotational constant [rotational kinetic energy $= BJ(J+1)$], so that J_i is no longer a good quantum number. For such a system in the quantum low-temperature regime ($k_B T \ll \hbar\omega_0$) the libron frequencies coincide with the classical frequencies of small oscillation. Accordingly, in Appendix A we derive the equations of motion for librons in a classical system[18] and clarify the relation between the quantum-mechanical systems where J_i is a good quantum number and classical systems (i.e., those where J_i is not a good quantum number). Contrary to the general problem of small oscillations, these two systems are only equivalent for lattice structures of sufficiently high symmetry. In particular, we find that the scaling relation between the frequencies of the two systems hold for the $Pa3$ structure but not for the C_{mmm} structure.

We now return to the case when J_i is a good quantum number, as applies to solid hydrogen. At first we shall treat the case when all molecules have $J = 1$. Within the $(J = 1)$ manifold it is con-

venient to use the operator equivalents introduced by Nakamura,[20]

$$O_i^0 = 3(J_{zi})^2 - 2, \tag{12a}$$

$$O_i^{\pm 1} = J_{zi}J_{\pm i} + J_{\pm i}J_{zi}, \tag{12b}$$

$$O_i^{\pm 2} = (J_{\pm i})^2, \tag{12c}$$

where $J_{\pm i} = J_{xi} \pm iJ_{yi}$. We wish to describe libron excitations assuming there are few such excitations present. Experimentally,[28,29] it is known that even at the transition temperature this assumption is a good one. Consequently, we expand about $J_{zi} = 0$. Previous authors[2-5] have generated such an expansion in various ways. For instance, Raich and Etters[4] introduce operators to simplify the Hamiltonian, but these operators are not exactly boson operators, so there are kinematic complications. In this connection it is interesting to note that for magnetic systems the correct behavior at low density of excitations out of the ground state is most readily recovered using diagrammatic methods.[30-32] For such calculations the simplest formalism utilizing pure bosons is not the Holstein-Primakoff[33] transformation, but rather the Dyson-Maleev[30,34] transformation. Although the latter leads to a formally non-Hermitian Hamiltonian, this circumstance creates no difficulties. Accordingly, in order to treat libron-libron interactions, we shall use this type of formalism. Thus, we take

$$O_i^0 = 3a_i^\dagger a_i + 3b_i^\dagger b_i - 2, \tag{13a}$$

$$O_i^1 = \sqrt{2}\,[a_i^\dagger - (1 - a_i^\dagger a_i - b_i^\dagger b_i)b_i\,], \tag{13b}$$

$$O_i^{-1} = \sqrt{2}[(1 - a_i^\dagger a_i - b_i^\dagger b_i)a_i - b_i^\dagger\,], \tag{13c}$$

$$O_i^2 = 2a_i^\dagger b_i, \tag{13d}$$

$$O_i^{-2} = 2a_i b_i^\dagger. \tag{13e}$$

In terms of these operators the Hamiltonian becomes

$$\mathcal{H} = E_0 + \mathcal{H}_0 + \sum_{n=3}^{6} V_n, \tag{14}$$

where E_0 is the Hartree ground-state energy, V_n is the perturbative term involving n boson operators, and $\mathcal{H}_0$ is the unperturbed Hamiltonian quadratic in the boson operators:

$$\begin{aligned}\mathcal{H}_0 = &-12\sum_{ij}\gamma_{ij}^{00}(a_i^\dagger a_i + b_i^\dagger b_i) + 2\sum_{ij}[\gamma_{ij}^{11}(a_i^\dagger - b_i)\\ &(a_j^\dagger - b_j) + (\gamma_{ij}^{11})^*(a_i - b_i^\dagger)(a_j - b_j^\dagger)\\ &+ \gamma_{ij}^{1,-1}(a_i^\dagger - b_i)(a_j - b_j^\dagger) + (\gamma_{ij}^{1,-1})^*(a_i - b_i^\dagger)\\ &\times(a_j^\dagger - b_j)] - 8\sum_{ij}[\gamma_{ij}^{20}a_i^\dagger b_i + (\gamma_{ij}^{20})^* a_i b_i^\dagger].\end{aligned} \tag{15}$$

Note that the linear term in the boson operators vanishes as a result of the assumed stability of the Hartree ground state. The terms V_3 and V_4 are given in Sec. IV where we consider the effects of libron-libron interactions. Since V_5 and V_6 lead to higher-order effects, we shall not consider them explicitly. The analysis of the excitation spectrum and thermodynamic properties can now be carried out in the usual way for a low-density Bose gas. In so doing, however, one tacitly assumes that the replacement of angular momentum operators by boson operators does not lead to significant errors due to the introduction of unphysical boson states. It is generally agreed that this assumption is a good one for the Heisenberg model of magnetic systems,[30] and we would expect it to be even better here, because of the presence of a large energy gap in the excitation spectrum.

The system we are considering is quite analogous to an antiferromagnet in that the zero-point deviations from the Hartree (Néel) state are small. Accordingly, the logical expansion parameter is the density of such excitations $\rho(T)$, and we expect to express quantities as series in the two parameters[15] $\rho(0)$ and $\rho(T) - \rho(0)$. Here, the thermal density of deviations $\rho(T) - \rho(0)$ is of order $\exp(-\Delta/k_B T)$, where Δ is the average libron-energy gap and the zero-point density of deviations $\rho(0)$ is of order $1/z$, where z is the number of nearest neighbors, or better, the cube of the range of the interaction. The appearance of $1/z$ as an expansion parameter is an indication of the fact that the molecular field becomes exact in the limit $z \to \infty$. The $1/z$ expansion for an antiferromagnet is described in Ref. 15 and is considered in more detail for the present problem in Sec. IV. In the remainder of this section we shall confine the discussion to the treatment of the quadratic Hamiltonian $\mathcal{H}_0$.

C. Equation of Motion for Librons

The first step in the calculation is to determine the approximate normal modes from the quadratic Hamiltonian $\mathcal{H}_0$. In this connection we note that exact diagonalization of $\mathcal{H}_0$ is virtually equivalent to the linearized equations of motion and , as is discussed in Appendix A, the resulting frequencies correspond (at least for the $Pa3$ structure) to the classical frequencies of small oscillations. Note that the additional approximation of keeping only those terms which conserve the total number of excitations [this "truncated" linear approximation is obtained by neglecting the terms in F' in Eq. (18), below] does not correspond to the classical problem of small oscillation (unless one eliminates displacements in certain "hard" directions). Thus it is not the "linear" approximation in the usual sense, e.g., in the sense of the linear theory of antiferromagnetic spin waves. There, keeping only the number conserving terms in the boson Hamiltonian leads to the dispersionless molecular-

field spectrum. We shall carry out the linear treatment here and shall evaluate approximately the lowest-order perturbation-theory corrections to the excitation spectrum in Sec. IV. A complete lowest-order calculation should be quite accurate, since corrections are of higher order in $1/z$.

In Eq. (15), it is convenient to introduce the following Fourier transforms:

$$a_\beta(\vec{k}) = N^{-1/2} \sum_{j(\beta)} a_{j(\beta)} \exp[-i\vec{k}\cdot\vec{R}_{j(\beta)}], \tag{16a}$$

$$b_\beta(\vec{k}) = N^{-1/2} \sum_{j(\beta)} b_{j(\beta)} \exp[-i\vec{k}\cdot\vec{R}_{j(\beta)}], \tag{16b}$$

$$\gamma^{mn}_{\alpha\beta}(\vec{k}) = \sum_{j(\beta)} \gamma^{mn}_{i(\alpha),j(\beta)} \exp\{-i\vec{k}\cdot[\vec{R}_{i(\alpha)} - \vec{R}_{j(\beta)}]\}, \tag{16c}$$

where α and β label the sublattices ($\alpha = 1, \ldots, s$, where s is the number of sublattices) and N is the number of unit cells, so that there are sN molecules in all. The sums in Eq. (16) are taken over all molecules i on a particular sublattice β. It follows that

$$\gamma^{-m,-n}_{\alpha\beta}(\vec{k}) = \gamma^{mn}_{\alpha\beta}(\vec{k})^* . \tag{17}$$

In terms of these Fourier transforms Eq. (15) becomes

$$\begin{aligned}\mathcal{H}_0 = \sum_{\vec{k}\mu\nu} [&a\delta_{\mu\nu} c^\dagger_\mu(\vec{k}) c_\mu(\vec{k}) + b\sigma_{\mu\nu} c^\dagger_\mu(\vec{k}) c_\nu(\vec{k}) \\ &+ F_{\mu\nu}(\vec{k}) c^\dagger_\mu(\vec{k}) c_\nu(\vec{k}) + \tfrac{1}{2} F'_{\mu\nu}(\vec{k}) c^\dagger_\mu(\vec{k}) c^\dagger_\nu(-\vec{k}) \\ &+ \tfrac{1}{2} F'_{\mu\nu}(\vec{k})^* c_\mu(\vec{k}) c_\nu(-\vec{k})],\end{aligned} \tag{18}$$

where $a = -12 \sum_\beta \gamma^{00}_{\mu\beta}(0)$ $\quad b = -8 \sum_\beta \gamma^{20}_{\mu\beta}(0)$.

For the $Pa3$ structure with only nearest-neighbor EQQ interactions, $a = 19\Gamma_0$. We shall assume that the different sites within the unit cell can be obtained from one another by rotations, in which case a and b are the same for all sublattices. Also we have introduced the operators $c_\mu(\vec{k})$ which are defined by

$$c_\alpha(\vec{k}) = a_\alpha(\vec{k}), \quad 1 \le \alpha \le s \tag{19a}$$

$$c_{s+\alpha}(\vec{k}) = b_\alpha(\vec{k}), \quad 1 \le \alpha \le s \tag{19b}$$

and the $(2s \times 2s)$ dimensional matrices $\underline{\sigma}$, $\underline{F}$, and $\underline{F}'$:

$$\underline{\sigma} = \begin{pmatrix} 0 & \underline{I} \\ \underline{I} & 0 \end{pmatrix} , \tag{20a}$$

$$\underline{F} = \begin{pmatrix} \underline{f} & -\underline{g} \\ -\underline{g}^* & \underline{f}^* \end{pmatrix} , \tag{20b}$$

$$\underline{F}' = \begin{pmatrix} \underline{g} & -\underline{f} \\ -\underline{f}^* & \underline{g}^* \end{pmatrix} , \tag{20c}$$

here $\underline{I}$ is the $(s \times s)$ unit matrix and $\underline{f}$ and $\underline{g}$ are also $(s \times s)$ matrices defined by

$$f_{\alpha\beta}(\vec{k}) = 4\gamma^{1,-1}_{\alpha\beta}(\vec{k}) , \tag{21a}$$

$$g_{\alpha\beta}(\vec{k}) = 4\gamma^{1}_{\alpha\beta}(\vec{k}) . \tag{21b}$$

In the linear approximation, i.e., treating $\mathcal{H}_0$ exactly, the normal modes are obtained from the equation of motion,

$$[c_\mu(\vec{k}), \mathcal{H}_0] = a c_\mu(\vec{k}) + b \textstyle\sum_\nu \sigma_{\mu\nu} c_\nu(\vec{k}) + \sum_\nu [F_{\mu\nu}(\vec{k}) c_\nu(\vec{k}) + F'_{\mu\nu}(\vec{k}) c^\dagger_\nu(-\vec{k})] , \tag{22a}$$

$$[c^\dagger_\mu(-\vec{k}), \mathcal{H}_0] = -a c^\dagger_\mu(-\vec{k}) - b \textstyle\sum_\nu \sigma_{\mu\nu} c^\dagger_\nu(-\vec{k}) - \sum_\nu [F_{\mu\nu}(\vec{k})^* c^\dagger_\nu(-\vec{k}) + F'_{\mu\nu}(\vec{k})^* c_\nu(\vec{k})] , \tag{22b}$$

where we have used the fact that the matrix $\underline{F}$ is Hermitian and $\underline{F}'$ is symmetric. In order to simplify the equations of motion we make use of the following relations between the matrices $\underline{F}$ and $\underline{F}'$:

$$\underline{F}'\underline{\sigma} = -\underline{F}, \tag{23a}$$

$$\underline{\sigma}\underline{F}' = -\underline{F}^* . \tag{23b}$$

The equations of motion now become

$$[c_\mu(\vec{k}), \mathcal{H}_0] = \textstyle\sum_\nu [a\delta_{\mu\nu} + b\sigma_{\mu\nu} + F_{\mu\nu}(\vec{k})] c_\nu(\vec{k}) - \sum_\nu F_{\mu\nu}(\vec{k}) \bar{c}^\dagger_\nu(-\vec{k}), \tag{24a}$$

$$[\bar{c}^\dagger_\mu(-\vec{k}), \mathcal{H}_0] = -\textstyle\sum_\nu [a\delta_{\mu\nu} + b\sigma_{\mu\nu} + F_{\mu\nu}(\vec{k})] \bar{c}^\dagger_\nu(-\vec{k}) + \sum_\nu F_{\mu\nu}(\vec{k}) c_\nu(\vec{k}), \tag{24b}$$

where $\bar{c}^\dagger_\mu(\vec{k}) = \textstyle\sum_\nu \sigma_{\mu\nu} c^\dagger_\nu(\vec{k})$. (25)

Taking linear combinations of Eqs. (24a) and (24b) we find that

$$[\{c_\mu(\vec{k}) + \bar{c}^\dagger_\mu(-\vec{k})\}, \mathcal{H}_0] = \textstyle\sum_\nu [a\delta_{\mu\nu} + b\sigma_{\mu\nu} + 2F_{\mu\nu}(\vec{k})]\{c_\nu(\vec{k}) - \bar{c}^\dagger_\nu(-\vec{k})\}, \tag{26a}$$

$$[\{c_\mu(\vec{k}) - \bar{c}^\dagger_\mu(-\vec{k})\}, \mathcal{H}_0] = \textstyle\sum_\nu [a\delta_{\mu\nu} + b\sigma_{\mu\nu}]\{c_\nu(\vec{k}) + \bar{c}^\dagger_\nu(-\vec{k})\}, \tag{26b}$$

and thus that

$$[[\{c_\mu(\vec{k}) - \bar{c}^\dagger_\mu(-\vec{k})\}, \mathcal{H}_0], \mathcal{H}_0] = \sum_{\nu\rho} [a\delta_{\mu\nu} + b\sigma_{\mu\nu}] \times [a\delta_{\nu\rho} + b\sigma_{\nu\rho} + 2F_{\nu\rho}(\vec{k})]\{c_\rho(\vec{k}) - \bar{c}^\dagger_\rho(-\vec{k})\} . \tag{27}$$

From Eq. (27) we conclude that the square of the eigenfrequencies ω^2 can be found by diagonalizing the matrix, $[a\underline{I} + b\underline{\sigma}][a\underline{I} + b\underline{\sigma} + 2\underline{F}]$:

$$\hbar^2\omega^2_\mu = [(a\underline{I} + b\underline{\sigma})(a\underline{I} + b\underline{\sigma} + 2\underline{F})]_\mu , \tag{28}$$

where the subscript μ denotes any eigenvalue of the matrix.

For the cases we consider in this paper, we have

$$[\underline{F}, b\underline{\sigma}] = 0, \tag{29}$$

TABLE II. Libron energies at $k=0$ in the $Pa3$ structure.

Experimental[a]		Theoretical[b]	
H_2	D_2	Nearest-neighbor EQQ interactions only[c]	All-neighbor EQQ interactions, nearest-neighbor non-EQQ interactions[d]
6.1 ± 0.5 cm^{-1}	8.3 ± 0.5 cm^{-1}	$10.4\Gamma_0$ (2)	$13.7\Gamma_0-2.0\epsilon_2+11.4\epsilon_0$ (2)
7.9 ± 0.5	11.4 ± 0.5	$14.3\Gamma_0$ (3)	$17.7\Gamma_0-6.9\epsilon_2+4.9\epsilon_0$ (3)
14.8 ± 1.0	21.2 ± 1.0	$26.2\Gamma_0$ (3)	$29.0\Gamma_0+0.01\epsilon_2+3.1\epsilon_0$ (3)

[a]Data are taken from Ref. 7. As discussed there, the two middle-frequency lines are combined for comparison with theory.

[b]Theoretical degeneracies are shown in parentheses.

[c]Results agree with those of Refs. 3–5.

[d]Results are perturbative and are valid when ϵ_0/Γ_0 and ϵ_2/Γ_0 are much less than unity. The results for EQQ interactions only were given in Ref. 6.

i.e., for the $Pa3$ structure $b=0$, and for the C_{mmm} structure $\underline{F}(k=0)$ is real. Since all the matrices commute, we can treat them as c numbers, i.e., they are simultaneously diagonalizable. Thus, we may rewrite Eq. (28) as

$$(\hbar\omega_\mu)^2=[(a\underline{I}+b\underline{\sigma}+\underline{F})^2-\underline{F}^2]_\mu. \tag{30}$$

If we denote by $\underline{u}$ the unitrary matrix which diagonalizes the commuting matrices $a\underline{I}+b\underline{\sigma}+\underline{F}$, and $\underline{F}$, then we may write

$$\sum_{\mu\nu} u^*_{\mu\rho}[a\delta_{\mu\nu}+b\sigma_{\mu\nu}+F_{\mu\nu}]u_{\nu\lambda}=\xi_\rho\delta_{\rho\lambda}, \tag{31a}$$

$$\sum_{\mu\nu} u^*_{\mu\rho}F_{\mu\nu}u_{\nu\lambda}=-\eta_\rho\delta_{\rho\lambda}, \tag{31b}$$

and if we define operators $d_\mu(\vec{k})$ and $\bar{d}^\dagger_\mu(-\vec{k})$ by

$$d_\mu(\vec{k})=\textstyle\sum_\nu u^*_{\nu\mu}(\vec{k})\,c_\nu(\vec{k}), \tag{32a}$$

$$\bar{d}^\dagger_\mu(-\vec{k})=\textstyle\sum_\nu u^*_{\nu\mu}(\vec{k})\,\bar{c}^\dagger_\nu(-\vec{k}), \tag{32b}$$

then Eqs. (24a) and (24b) become

$$[d_\mu(\vec{k}),\,\mathcal{H}_0]=\xi_\mu d_\mu(\vec{k})+\eta_\mu\bar{d}^\dagger_\mu(-\vec{k}), \tag{33a}$$

$$[\bar{d}^\dagger_\mu(-\vec{k}),\,\mathcal{H}_0]=-\xi_\mu\bar{d}^\dagger_\mu(-\vec{k})-\eta_\mu d_\mu(\vec{k}). \tag{33b}$$

Finally, we perform the Bogoliubov transformation[33] to the elementary excitation operators of the system $f_\mu(\vec{k})$ and $\bar{f}^\dagger_\mu(-\vec{k})$:

$$d_\mu(\vec{k})=\alpha_\mu(\vec{k})f_\mu(\vec{k})+\beta_\mu(\vec{k})\bar{f}^\dagger_\mu(-\vec{k}), \tag{34a}$$

$$\bar{d}^\dagger_\mu(-\vec{k})=\beta_\mu(\vec{k})f_\mu(\vec{k})+\alpha_\mu(\vec{k})\bar{f}^\dagger_\mu(-\vec{k}), \tag{34b}$$

where

$$\alpha_\mu(\vec{k})=[(\xi_\mu+\hbar\omega_\mu)/2\hbar\omega_\mu]^{1/2}, \tag{35a}$$

$$\beta_\mu(\vec{k})=-[(\xi_\mu-\hbar\omega_\mu)/2\hbar\omega_\mu]^{1/2}, \tag{35b}$$

$$\hbar\omega_\mu=(\xi^2_\mu-\eta^2_\mu)^{1/2}. \tag{35c}$$

We have carried out numerical and analytic calculations of the libron spectrum at zero wave vector for both the $Pa3$ and C_{mmm} structures. As previously noted,[6] it is very important to include the effects of next-nearest-neighbor interactions. In Tables II and III, we give our results, including all-neighbor interactions as well as those for nearest-neighbor interactions only, for comparison. Since the EQQ interactions are dominant, we have included the other interactions perturbatively,

TABLE III. Libron energies at $k=0$ in the C_{mmm} structure.

Experimental[a]		Theoretical[b]	
H_2	D_2	Nearest-neighbor EQQ interactions only	All-neighbor EQQ interactions, nearest-neighbor non-EQQ interactions[c]
6.3 ± 0.5 cm^{-1}	8.8 ± 0.5 cm^{-1}	$12.6\Gamma_0$ (2)	$7.9\Gamma_0-3.6\epsilon_2+1.4\epsilon_0$ (2)
10.8 ± 0.5	14.4 ± 0.5	$24.8\Gamma_0$ (1)	$20.2\Gamma_0-4.8\epsilon_2+11.2\epsilon_0$ (1)
14.8 ± 1.0	21.2 ± 1.0	$33.6\Gamma_0$ (1)	$28.5\Gamma_0+3.8\epsilon_2+3.8\epsilon_0$ (1)

[a]Data are taken from Ref. 7. As discussed in the text, the two lowest-frequency lines are combined for comparison with theory.

[b]Theoretical degeneracies are shown in parentheses.

[c]Results are perturbative and are valid when ϵ_0/Γ_0 and ϵ_2/Γ_0 are much less than unity.

obtaining the results given in the last column of Tables II and III. Finally, it should be emphasized that the relatively large effects of zero-point motion, performed in Sec. IV, are not included in these tables. We shall discuss the significance of these results in Sec. V, where we compare the calculations of both the libron frequencies and the Raman intensities with the observed Raman spectra.

III. FORMULA FOR RAMAN INTENSITIES

In this section, we shall calculate the Raman scattering amplitudes using the polarizability approximation.[17] That is, we shall assume that the polarizability of the solid can be expressed as the sum of molecular polarizabilities $\overleftrightarrow{\alpha}(i)$:

$$\overleftrightarrow{\alpha} = \sum_i \overleftrightarrow{\alpha}(i), \tag{36}$$

where $\overleftrightarrow{\alpha}(i)$ is the polarizability tensor of the molecule situated at lattice site i. The interaction of the electromagnetic field with the system can then be written in the form

$$\mathcal{H}_{\rm int} = \tfrac{1}{2}\sum_i \vec{E}\cdot\overleftrightarrow{\alpha}(i)\cdot\vec{E}, \tag{37}$$

where $\vec{E}$ is the externally applied oscillating electric field.

It is convenient to rewrite Eq. (37) in terms of spherical components[21] as

$$\mathcal{H}_{\rm int} = \tfrac{1}{2}\sum_i \sum_{\mu\nu} C(112;\ \mu,\ \nu) \times \alpha^{(2)}_{\mu+\nu}(i)^* E_\mu E_\nu + \tfrac{1}{2}\bar{\alpha}E^2, \tag{38}$$

where $\alpha^{(2)}_\rho(i)$ is a second-rank tensor with components

$$\alpha^{(2)}_{\pm 2} = \tfrac{1}{2}(\alpha_{xx} - \alpha_{yy} \pm 2i\,\alpha_{xy}), \tag{39a}$$

$$\alpha^{(2)}_{\pm 1} = \mp(\alpha_{xz} \pm i\,\alpha_{yz}), \tag{39b}$$

$$\alpha^{(2)}_0 = (6)^{-1/2}(2\alpha_{zz} - \alpha_{xx} - \alpha_{yy}), \tag{39c}$$

and $\bar{\alpha}$ is defined as

$$\bar{\alpha} = \tfrac{1}{3}(\alpha_{xx} + \alpha_{yy} + \alpha_{zz}). \tag{40}$$

The second term of Eq. (38) will not contribute to the phenomenon of interest and will henceforth be neglected. In Eq. (38) the spherical components of the tensors are referred to an arbitrary set of axes, which we take as the crystal axes and which we refer to as $\hat{c}$. Since the expression for the polarizability tensor assumes its simplest form when referred to an axis fixed in the molecule, viz., the principal axis $\hat{n}$, we write

$$\alpha^{(2)}_\rho(i)_{\hat{c}} = \sum_\lambda D^{(2)}_{\rho\lambda}(\alpha_i, \beta_i, \gamma_i)^*\, \alpha^{(2)}_\lambda(i)_{\hat{n}}, \tag{41}$$

where $\alpha^{(2)}_\lambda(i)$ is the polarizability tensor for molecule i, the outermost unit-vector subscript indicates the quantization axis, and $(\alpha_i, \beta_i, \gamma_i)$ are the Euler angles specifying the orientation of the principal axes relative to the crystal axes. Now $\alpha^{(2)}_\lambda(i)_{\hat{n}}$ is nonvanishing only for $\lambda = 0$:

$$\alpha^{(2)}_\lambda(i)_{\hat{n}} = \delta_{\lambda 0}(\alpha_{\parallel} - \alpha_{\perp})(\tfrac{2}{3})^{1/2} \equiv \delta_{\lambda 0}(6)^{1/2} K\bar{\alpha}, \tag{42}$$

where K is the anisotropy of the polarizability. Thus Eq. (41) becomes

$$\alpha^{(2)}_\rho(i)_{\hat{c}} = (6)^{1/2} K\bar{\alpha}\, D^{(2)}_{\rho 0}(\alpha_i, \beta_i, \gamma_i)^* = (8\pi/15)^{1/2} 3K\bar{\alpha}\, Y^\rho_2(\beta_i, \alpha_i). \tag{43}$$

In order to find the change in the polarizability as the molecule rotates due to libron excitations, it is convenient to express $\overleftrightarrow{\alpha}$ in terms of coordinates referred to the orientations in the Hartree ground state. Using the rotation matrices $D^{(2)}_{\rho\lambda}$ we may rewrite Eq. (43) as

$$\alpha^{(2)}_\rho(i)_{\hat{c}} = 3K\bar{\alpha}(\tfrac{8}{15}\pi)^{1/2} \times \sum_\gamma D^{(2)}_{\rho\gamma}(\chi_i)^* Y^\gamma_2(\omega_i), \tag{44}$$

where ω_i specifies the orientation of molecule i relative to its equilibrium value, and χ_i are the Euler angles specifying the equilibrium orientation for the ith molecule relative to the crystal axes. This result enables us to write the interaction Hamiltonian of Eq. (38) as

$$\mathcal{H}_{\rm int} = 3K\bar{\alpha}(\tfrac{8}{15}\pi)^{1/2} \times \sum_{i(\alpha),\alpha} \sum_{\mu\nu\lambda} C(112;\mu,\nu) D^{(2)}_{\mu+\nu,\lambda}(\chi_{i(\alpha)}) \times Y^\lambda_2(\omega_{i(\alpha)})^* E_\mu(i(\alpha)) E_\nu(i(\alpha)), \tag{45}$$

where $E_\mu(i(\alpha))$ is the μth component (referred to the crystal axes) of the externally applied electric field at the position of the molecule in the ith unit cell and on the αth sublattice.

The process we are considering is the following[7]: A photon of wave vector $\vec{k}$ and polarization τ impinges on the system and an emitted photon of wave vector $\vec{k}'$ and polarization τ' is observed. As a result, a libron of wave vector $\vec{q} = \vec{k} - \vec{k}'$ and in the branch σ of the libron spectrum is created in the system. The electric field can be written in terms of photon creation and annihilation operators $\alpha^\dagger_{\vec{k},\tau}$ and $\alpha_{\vec{k},\tau}$ as[35]

$$\vec{E}(\vec{r}, t) = i\sum_{\vec{k},\tau}(4\pi\hbar\omega_{\vec{k},\tau}/2V)^{1/2}\hat{\epsilon}(\vec{k},\tau) \times \{\alpha_{\vec{k},\tau}\exp[i(\vec{k}\cdot\vec{r} - \omega_{\vec{k},\tau}t)] - \alpha^\dagger_{\vec{k},\tau}\exp[-i(\vec{k}\cdot\vec{r} - \omega_{\vec{k},\tau}t)]\}, \tag{46}$$

where $\hat{\epsilon}(\vec{k},\tau)$ is the unit polarization vector describing the photon mode of wave vector $\vec{k}$ and polarization τ with

$$\vec{k}\cdot\hat{\epsilon}(\vec{k},\tau) = 0. \tag{47}$$

The calculation of the Raman intensities at es-

sentially zero temperature requires the determination of the matrix element $|\langle f|\mathcal{H}_{\rm int}|i\rangle|$ where the initial state $|i\rangle$ is that state with one photon in the mode $(\vec{k}, \tau)$ and no librons; the final state $|f\rangle$ is that state with one photon of mode $(\vec{k}', \tau')$ and one libron with wave vector $\vec{q}$ and of branch σ.[36] Denoting the relative intensity of an excitation of a $(\vec{q}, \sigma)$ libron by I_σ, we find that

$$\begin{aligned} I_\sigma = \sum_{\alpha\beta}\sum_{i(\alpha)}\sum_{j(\beta)}\sum_{\mu\nu\mu'\nu'}\sum_{\lambda\lambda'\tau\tau'} & C(112;\mu,\nu) \\ & \times C(112;\mu',\nu')\,\epsilon_\mu(\vec{k},\tau)\,\epsilon_\nu(\vec{k}',\tau') \\ & \times \epsilon_{\mu'}(\vec{k},\tau)^*\,\epsilon_{\nu'}(\vec{k}',\tau')^* D^{(2)}_{\mu+\nu,\lambda}(\chi_{i(\alpha)}) \\ & \times D^2_{\mu'+\nu',\lambda'}(\chi_{j(\beta)})^* \exp[i(\vec{k}-\vec{k}')\cdot(\vec{R}_{i(\alpha)}-\vec{R}_{j(\beta)})] \\ & \times \langle 0|\,Y^{\lambda'}_2(\omega_{j(\beta)})\,|\vec{q},\sigma\rangle\langle\vec{q},\sigma|\,Y^{\lambda}_2(\omega_{i(\alpha)})^*\,|0\rangle, \end{aligned} \tag{48}$$

where $|0\rangle$ is the state with no librons and $|\vec{q},\sigma\rangle$ is a state with one libron of wave vector $\vec{q}$ in the σ branch. The sum over τ and τ' arises from averaging over initial photon polarizations and summing over final photon polarizations. Here $\epsilon_\mu(\vec{k},\tau)$ is the μth component (referred to the crystal axes) of the polarization vector $\hat{\epsilon}(\vec{k},\tau)$. Using Eq. (47), we may write

$$\begin{aligned} \sum_{\tau\tau'} \epsilon_\mu(\vec{k},\tau)\,\epsilon_{\mu'}(\vec{k},\tau)^*\,\epsilon_\nu(\vec{k}',\tau')\,\epsilon_{\nu'}(\vec{k}',\tau')^* \\ = [\delta_{\mu\mu'} - \hat{k}_\mu \hat{k}^*_{\mu'}]\,[\delta_{\nu\nu'} - \hat{k}'_\nu k'^*_{\nu'}]\,, \end{aligned} \tag{49}$$

where $\hat{k}$ and $\hat{k}'$ are unit vectors in the direction of the incident and scattered photons, respectively.

The expression for the intensity is greatly simplified if the sample used is a powder, as we shall now assume. To facilitate the calculation we use the fact that the spherical components of a unit-vector transform under rotations as a first-rank tensor.[21] Hence, we can write

$$\hat{k}'_\mu = \textstyle\sum_\nu D^{(1)}_{\mu\nu}(\chi)^*\,\xi'_\nu, \tag{50}$$

where ξ'_ν is the νth component of $\hat{k}'$ with respect to an axis fixed in the laboratory frame and χ denotes the Euler angles of the laboratory frame with respect to the crystal axes. For convenience we take the laboratory frame to have its z axis along the direction of the incident photon. Denoting powder averages by $\langle\cdots\rangle_{\rm av}$, we write

$$\langle \hat{k}'_\mu \hat{k}'^*_\nu\rangle_{\rm av} = \sum_{\rho\rho'} \langle D^{(1)}_{\mu\rho}(\chi)^* D^{(1)}_{\nu\rho'}(\chi)\rangle_{\rm av}\,\xi_\rho \xi^*_{\rho'}. \tag{51}$$

We have[21]

$$\langle D^{(J)}_{\mu\rho}(\chi)^* D^{(J')}_{\nu\rho'}(\chi)\rangle_{\rm av} = (2J+1)^{-1}\,\delta_{\mu\nu}\,\delta_{\rho\rho'}\,\delta_{JJ'}, \tag{52}$$

which yields the obvious result

$$\langle \hat{k}'_\mu k'^*_\nu\rangle_{\rm av} = \tfrac{1}{3}\delta_{\mu\nu}. \tag{53}$$

Similarly, we may write

$$\begin{aligned} \langle \hat{k}_\mu \hat{k}^*_{\mu'} \hat{k}'_\nu \hat{k}'^*_{\nu'}\rangle_{\rm av} = \sum_{\alpha\beta\gamma\rho} \xi_\alpha \xi^*_\beta \xi'_\gamma \xi'^*_\rho \\ \times \langle D^{(1)}_{\mu\alpha}(\chi)^* D^{(1)}_{\mu'\beta}(\chi)\, D^{(1)}_{\nu\gamma}(\chi)^* D^{(1)}_{\nu'\rho}(\chi)\rangle_{\rm av}, \end{aligned} \tag{54}$$

where $\hat{k}'$ and $\vec{\xi}'$ refer to the scattered photon. Using the Clebsch-Gordan series and Eq. (52) we find that

$$\begin{aligned} \langle \hat{k}_\mu \hat{k}^*_{\mu'} \hat{k}'_\nu \hat{k}'^*_{\nu'}\rangle_{\rm av} = \delta_{\mu+\nu,\ \mu'+\nu'} \textstyle\sum_J (2J+1)^{-1} \\ \times C(11J;\mu,\nu)\,c(11J;\mu',\nu') \\ \times \textstyle\sum_\rho C(11J;0,\rho)^2 |\,\xi'_\rho\,|^2. \end{aligned} \tag{55}$$

These results enable us to write the relative intensities in the form

$$\begin{aligned} I_\sigma = C^0 \sum_{\lambda\lambda'\alpha\beta}\sum_{i(\alpha)\ j(\beta)} & D^{(2)}_{\lambda\lambda'}(\omega_{\alpha\beta})^* \\ & \times \langle\vec{q}\,\sigma|\,Y^{\lambda}_2(\omega_{i(\alpha)})^*\,|0\rangle\langle 0|\,Y^{\lambda'}_2(\omega_{j(\beta)})\,|\vec{q},\sigma\rangle \\ & \times \exp[i\vec{q}\cdot(\vec{R}_{i(\alpha)} - \vec{R}_{j(\beta)})], \end{aligned} \tag{56}$$

where $\omega_{\alpha\beta}$ are the Euler angles specifying the equilibrium axes of molecules on sublattice β relative to the equilibrium axes of molecules on sublattice α, and C^0 is a weak function of the angle between $\hat{k}$ and $\hat{k}'$. The matrix elements $\langle 0|\,Y^{\lambda'}_2(\omega_{j(\beta)})\,|\vec{q},\sigma\rangle$ are found by expressing $Y^{\lambda'}_2(\omega_{j(\beta)})$ in terms of the excitation operators f_ρ and $\bar{f}^\dagger_\rho$ of the system. Thus we arrive, finally, at the expression for the Raman intensities in terms of the eigenvectors of the dynamical matrix:

$$\begin{aligned} I_\sigma = (\alpha_\sigma - \beta_\sigma)^2 \\ \times \sum_{\mu\nu}\sum_{m,m'=\pm1} D^{(2)}_{-m,-m'}(\omega_{\mu\nu})^*\,U^{(m)*}_{\mu\sigma} U^{(m')}_{\nu\sigma}. \end{aligned} \tag{57}$$

Here the subscripts μ and ν are summed over the range $(1, s)$ and σ is the mode index $1 \le \sigma \le 2s$. Also $\underline{U}^{(m)}$ is the $(s\times 2s)$ rectangular array defined by setting

$$\underline{u} = \begin{pmatrix} \underline{U}^{(1)} \\ \underline{U}^{(-1)} \end{pmatrix}. \tag{58}$$

IV. ZERO-POINT MOTION AND LIBRON-LIBRON INTERACTIONS

In this section, we shall discuss the effects of zero-point motion and libron-libron interactions. The diagrammatic formulation of perturbation theory which we shall use is that due to Bloch and deDominicis.[37] From their formulation, it is quite apparent that for each hole line in any diagram there corresponds a Bose factor which is approximately

$$\rho(T) - \rho(0) = [\exp(\Delta/k_B T) - 1]^{-1},$$

where Δ is the average libron energy gap. This factor is quite small and hence, except perhaps very near the transition temperature, these temperature-dependent terms will be dominated by the zero-temperature effects.

To study these effects we need consider only diagrams with no hole lines. We shall further simplify the calculations through the use of the $1/z$ expansion,[15] where z is the number of nearest neighbors. Formally, this expansion is generated by taking the unperturbed Hamiltonian to consist of the molecular field terms in $\mathcal{H}_0$, i.e., those terms diagonal in the number of excitations. We write these terms as

$$\mathcal{H}_{00} = \hbar\omega_0 \sum_i (a_i^\dagger a_i + b_i^\dagger b_i), \tag{59}$$

where $\hbar\omega_0 \equiv 19\Gamma_0 \equiv E_0$, and is considered to be of order z, because z nearest neighbors contribute to this field. (In a more refined calculation $\hbar\omega_0$ should include the effect of further-neighbor interactions and of anharmonic shifts. As we shall discuss in a separate paper, these effects tend to cancel, and $\hbar\omega_0$ remains close to the unperturbed value used here.) The perturbation then consists of the quadratic "transfer" terms, the quadratic "pair-creation" terms, and the higher-order anharmonic terms. Terms in perturbation theory are classified according to their order in $1/z$ as follows: As mentioned above, E_0 is considered to be of order z; sums over n independent lattice sites are considered to be of order z^n. Ordinarily, one can infer the concentration dependence of perturbative contributions by similar reasoning. In fact, it is easy to see that z and x always appear in the combination (zx). This point of view is closely related to that of Nakamura,[16] and hence, our calculation of the thermodynamic properties will be abbreviated.

To calculate $\langle O_i^0 \rangle$, or equivalently, $\langle a_i^\dagger a_i + b_i^\dagger b_i \rangle$ at zero temperature, we use Feynman's theorem to write

$$Nsx\langle a_i^\dagger a_i + b_i^\dagger b_i \rangle = \frac{-\partial F}{\partial(\hbar\omega_0)}, \tag{60}$$

where F is the free energy. Hence, a calculation of F to lowest order in $1/z$ will lead directly to an evaluation of $\langle O_i^0 \rangle$. To lowest order in $1/z$, only the quadratic terms describing pair creation contribute to the free energy at zero temperature. Thus to lowest order in $1/z$, the energy is that of the linear theory, but our formulation is rather simple in that summations over the Brillouin zone are avoided. Using second-order perturbation theory we find the free energy correct to second order to be

$$F = -\tfrac{1}{3}NE_0sx^2 - 8Nsx \times \sum_j (|\gamma_{ij}^{11}|^2 + |\gamma_{ij}^{1,-1}|^2)/\hbar\omega_0 \tag{61}$$

at zero temperature. Then Eq. (60) yields

$$\langle a_i^\dagger a_i + b_i^\dagger b_i \rangle = 8x^{-1}E_0^{-2} \sum_j (|\gamma_{ij}^{11}|^2 + |\gamma_{ij}^{1,-1}|^2), \tag{62}$$

in agreement with Nakamura's result[16] for $x = 1$. The values of the coefficients $\gamma_{ij}^{mm'}$ are discussed and tabulated in Appendix B. Using the values of Table VII, we obtain the numerical results, neglecting the very small effects of further-neighbor interactions,

$$F/(-\tfrac{1}{3}NE_0sx^2) = 1 + 0.049x^{-1}, \tag{63}$$

$$\langle 1 - \tfrac{3}{2}J_{zi}^2 \rangle = 1 - 0.025x^{-1}. \tag{64}$$

Next let us evaluate the lowest order (in $1/z$) corrections to the libron spectrum. Strictly speaking, the perturbations to the libron spectrum are described by the self-energy, $\Sigma(\vec{k}, \sigma, \omega)$, where σ is the mode index and ω the frequency, or, equivalently, since we take the unperturbed Hamiltonian to be diagonal in real space, $\Sigma(\vec{R}, \vec{R}'; \sigma, \sigma'; \omega)$. The off-diagonal terms in Σ due to the quadratic perturbations give rise to the dispersion in the libron spectrum found within the linear theory used in the main body of this paper. Here we wish to estimate the effect of libron-libron interactions on the excitation spectrum. For this purpose it is convenient to neglect the dispersion of the linear libron spectrum. In other words, we shall calculate only the average over all modes and momentum space of the energy shift due to libron-libron interactions. Thus, we shall calculate $\Sigma(\vec{R}, \vec{R}; \sigma, \sigma; \omega)$. By symmetry, this function is independent of both $\vec{R}$ and σ. The shift in the libron frequency $\Delta\omega$ is then obtained by evaluating Σ for $\omega = \omega_0$:

$$\hbar\Delta\omega = \sum (\vec{R}, \vec{R}; \sigma, \sigma; \omega_0). \tag{65}$$

Since we are only interested in the effect of the anharmonic terms, we wish to evaluate the lowest-order terms in perturbation theory involving the cubic and quartic anharmonic terms. Terms involving more than four operators can be shown to be of higher order in $1/z$. Had we not chosen the Dyson-Maleev representation, we would have had to evaluate many more terms. The sum of all such extra terms must vanish, of course. Such a cancellation has been shown to occur in the antiferromagnet.[38] The restriction to diagrams with no hole lines drastically reduces the number of terms one must examine. For instance, only terms of the type shown in Figs. 1(a) and 1(b) contribute to first order in $1/z$. Diagrams of the type shown in Fig. 1(c), where the quartic vertex conserves the number of particles, do not contribute at zero temperature, because they require the presence of a hole line.

For an explicit calculation we need to write down the cubic and quartic perturbations. For the $Pa3$ structure, we have

$$V_3 = 6\sqrt{2}\sum_{ij}[\gamma_{ij}^{01}(a_i^\dagger a_i + b_i^\dagger b_i)(a_j^\dagger - b_j) + (\gamma_{ij}^{01})^*(a_i^\dagger a_i + b_i^\dagger b_i)(a_j - b_j^\dagger)] + 4\sqrt{2}\sum_{ij}[\gamma_{ij}^{12}(a_i^\dagger - b_i)a_j^\dagger b_j + \gamma_{ij}^{1;-2}(a_i^\dagger - b_i)a_j b_j^\dagger + (\gamma_{ij}^{12})^*(a_i - b_i^\dagger)a_j b_j^\dagger + (\gamma_{ij}^{1;-2})^*(a_i - b_i^\dagger)a_j^\dagger b_j] \quad (66a)$$

and

$$V_4 = 9\sum_{ij}\gamma_{ij}^{00}(a_i^\dagger a_i + b_i^\dagger b_i)(a_j^\dagger a_j + b_j^\dagger b_j) + 12\sum_{ij}[\gamma_{ij}^{02}(a_i^\dagger a_i + b_i^\dagger b_i)a_j^\dagger b_j + (\gamma_{ij}^{02})^*(a_i^\dagger a_i + b_i^\dagger b_i)a_j b_j^\dagger] + 4\sum_{ij}[\gamma_{ij}^{11}(a_i^\dagger - b_i)(a_j^\dagger a_j + b_j^\dagger b_j)b_j - (\gamma_{ij}^{11})^*(a_i - b_i^\dagger)(a_j^\dagger a_j + b_j^\dagger b_j)a_j] + 4\sum_{ij}[(\gamma_{ij}^{1;-1})^*(a_i - b_i^\dagger)(a_j^\dagger a_j + b_j^\dagger b_j)b_j - \gamma_{ij}^{1;-1}(a_i^\dagger - b_i)(a_j^\dagger a_j + b_j^\dagger b_j)a_j] + 4\sum_{ij}[\gamma_{ij}^{22}a_i^\dagger b_i a_j^\dagger b_j + (\gamma_{ij}^{22})^* a_i b_i^\dagger a_j b_j^\dagger + \gamma_{ij}^{2;-2}a_i^\dagger b_i a_j b_j^\dagger + (\gamma_{ij}^{2;-2})^* a_i b_i^\dagger a_j^\dagger b_j]. \quad (66b)$$

Using these forms we find that

$$\hbar\Delta\omega = -16E_0^{-1}\sum_j\{[9|\gamma_{ij}^{01}|^2 + 2|\gamma_{ij}^{1;-2}|^2 + 2|\gamma_{ij}^{12}|^2] - [\tfrac{3}{2}|\gamma_{ij}^{11}|^2 + \tfrac{3}{2}|\gamma_{ij}^{1;-1}|^2]\}, \quad (67)$$

where the terms in the first square bracket are the contributions from the cubic terms of the type shown in Fig. 1 (a), which we denote as $\hbar\Delta\omega_{3\text{-}3}$, and the terms in the second square bracket are those from the quartic perturbations shown in Fig. 1 (b), which we denote as $\hbar\Delta\omega_{4\text{-}2}$. Using Table VII, we find

$$\hbar\Delta\omega_{3\text{-}3} = -4.46\Gamma_0, \quad (68a)$$

$$\hbar\Delta\omega_{4\text{-}2} = 0.94\Gamma_0, \quad (68b)$$

$$\hbar\Delta\omega = -3.52\Gamma_0 = -0.186E_0. \quad (68c)$$

For the pure ($J = 1$) solid we can summarize our calculation by saying that on the average, the effect of anharmonicity is to modify the linear spectrum by effectively replacing Γ_0 by $\xi_{\text{rot}}\Gamma_0$, where

$$\xi_{\text{rot}} = (1 - 0.186) = 0.814. \quad (68d)$$

Let us make two comments about this result. First of all, note that the expression in Eq. (67) involves a lattice sum over one independent site ($\sim zx$) and one energy denominator $(E_0)^{-1} \sim (zx)^{-1}$, so that $\hbar\Delta\omega$ is independent of zx. Second, note that the correction to the average libron excitation energy is very large, viz., of order 15%, which might be surprising in view of the smallness of the static zero-point effects. This energy shift involves anharmonicity which is essentially unrelated to the other zero-point effects and which therefore need not be small. Since this energy shift is quite large, we are presently performing detailed calculations of the energy shifts of the individual libron modes. Also, we expect that this strong anharmonicity is probably responsible for the anomalous width of the highest-energy libron excitation observed by Hardy *et al.*[7] Calculation of this effect is also in progress.

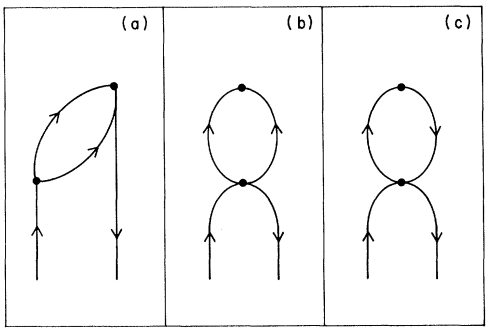

FIG. 1. Diagrams representing lowest-order (in $1/z$) corrections to the unperturbed libron spectrum. Here upward-going lines represent particles and downward-going lines represent holes. Only (a) and (b) contribute at zero temperature. Diagrams such as (c) do not contribute at zero temperature.

V. DISCUSSION AND SUMMARY

A. Discussion

Let us now interpret the results of our calculations. It is clear from the Raman studies that solid hydrogen is not described accurately by the model which has been used. Either the crystal structure is somewhat different from those we have considered, or the model of rotational excitations in a *rigid* lattice is not valid.

In order to compare our calculations with the experimental data, we therefore assume that two of the observed lines in the Raman spectrum arise from a single line in the rigid undistorted lattice.[8] Presumably, then, when distortions or libron-phonon coupling is taken into account the observed spectrum may be reproduced. [*Note added in proof*. The discussion in this section has become obsolete. Since submission of this manuscript further experimental data has been reported by Nakamura. He has proposed that the lowest three lines in the Raman spectrum should be associated with the single libron modes. The remaining two lines were attributed to two-libron processes, although no reasonable mechanism was advanced. We have used the anharmonicity to obtain such a mechanism. Including anharmonic shifts as in

TABLE IV. Raman intensities for the $Pa3$ structure.

Experimental[a]				Theoretical[b]		
H_2 Frequency (cm^{-1})	Relative intensity	D_2 Frequency (cm^{-1})	Relative intensity	Nearest-neighbor truncated linear theory[c]	Nearest-neighbor full linear theory	All-neighbor full linear theory
6.1 ± 0.5	1.00	8.3 ± 0.5	1.00	1.00	1.00	1.00
7.1 ± 0.5, 10.8 ± 0.5 } 7.9 ± 0.5[d]	0.18, 0.05 } 0.23[d]	10.3 ± 0.5, 14.4 ± 0.5 } 11.4 ± 0.5[d]	0.34, 0.12 } 0.46[d]	0.413	0.300	0.317
14.8 ± 1.0	0.13	21.2 ± 1.0	0.20	0.087	0.034	0.041

[a]See Ref. 7.
[b]Theoretical intensities are calculated from Eq. (57) assuming only EQQ interactions.
[c]Here truncated means that the terms in $\underline{F}'$ in Eq. (18) are dropped. These results were given in Ref. 7.
[d]As discussed in Ref. 7, we combine the two middle-frequency lines for comparison with theory.

Eq. (68) we have obtained an excellent fit to the entire five-line spectrum. The details of this calculation will be published shortly.] In Tables IV and V, we compare the calculated and observed intensities in this way. Note that for the C_{mmm} structure, the excitation at the lowest energy is doubly degenerate. Accordingly it is necessary to associate the two observed absorptions at lowest energy with this excitation. As can be seen, the correlation between the observed and calculated intensities is rather poor for the C_{mmm} structure. In particular, we find that creation of the highest-energy libron mode in a Raman process is forbidden by symmetry for this structure. For the $Pa3$ structure, the situation is much better. Following the symmetry argument of Hardy *et al.*,[7] we have associated the two absorptions at intermediate energy with the single excitation calculated on the basis of the rigid-lattice model. As can be seen from Figs. 2–5, the intensities calculated for the $Pa3$ structure are indeed in much better agreement with experiment than those calculated for the C_{mmm} structure. Although this discussion is based on calculations for which $\epsilon_0 = \epsilon_2 = 0$, it is clear that for small values of these parameters our results should remain qualitatively valid.

Let us next discuss the frequencies of the libron excitations. In fitting the observed Raman spectrum it is not reasonable to vary the parameters ϵ_0 and ϵ_2 arbitrarily. Although we do not regard the theoretical estimates as being conclusive, we do not wish to invoke values of ϵ_0 and ϵ_2 which would disturb the rather good agreement between theory and experiment which is obtained for such quantities as the specific heat,[39,40] $(\partial p/\partial T)_V$,[29,41] or the NMR spectrum.[42] To make this discussion quantitative note that the aforementioned experiments depend most sensitively on (1) the rms value of the

TABLE V. Raman intensities for the C_{mmm} structure.

Experimental[a]				Theoretical[b]		
H_2 Frequency (cm^{-1})	Relative intensity	D_2 Frequency (cm^{-1})	Relative intensity	Nearest-neighbor truncated linear theory[c]	Nearest-neighbor full linear theory	All-neighbor full linear theory
6.1 ± 0.5, 7.1 ± 0.5 } 6.3 ± 0.5[d]	0.85, 0.15 } 1.00[d]	8.3 ± 0.5, 10.3 ± 0.5 } 8.8 ± 0.5[d]	0.75, 0.25 } 1.00[d]	1.00	1.00	1.00
10.8 ± 0.5	0.042	14.4 ± 0.5	0.09	1.00	0.680	0.542
14.8 ± 1.0	0.110	21.2 ± 1.0	0.15	Not allowed • • •		

[a]See Ref. 7.
[b]Theoretical intensities are calculated from Eq. (57) assuming only EQQ interactions.
[c]Here truncated means that the terms in $\underline{F}'$ in Eq. (18) are dropped.
[d]As discussed in the text, we combine the two low-frequency lines for comparison with theory.

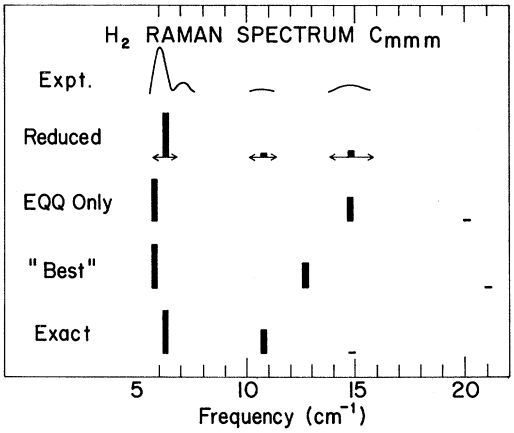

FIG. 2. Fit to the Raman data of Ref. 7 for solid H_2 assuming the C_{mmm} structure. The intensity is plotted in the vertical direction. The reduced experimental data is the result of combining the experimental lines (denoted expt) as in Tables IV and V, and the arrows indicate the error range. The "best" fit is the best fit which can be obtained subject to the restriction that $|\epsilon_0| \leq 0.20$ cm^{-1} and $|\epsilon_2| \leq 0.20$ cm^{-1}. The exact fit is that which exactly reproduces the reduced experimental data. The values (in cm^{-1}) of the parameters used for the various fits are EQQ only: $\Gamma_{\text{expt}} = 0.734$; "best" fit: $\Gamma_{\text{expt}} = 0.79$, $\epsilon_2 = 0.20$, $\epsilon_0 = -0.20$; and exact fit: $\Gamma_{\text{expt}} = 0.439$, $\epsilon_2 = 0.742$, $\epsilon_0 = 0.14$. We have indicated the forbidden transition in the C_{mmm} structure at high frequency (see Table V) by a vertical bar of ~ zero height.

energy

$$(E_{\text{rms}})^2 \equiv \text{Tr}(H_{ij})^2/\text{Tr}1$$

or (2) the energy ΔE of the first excited state of the isolated pair of ($J = 1$) molecules. It is therefore of interest to examine how strongly these quantities depend on ϵ_0 and ϵ_2. For ΔE, we have, from Ref. 25,

$$\Delta E = 4\Gamma_0 - \tfrac{1}{10}(\epsilon_0 + 2\epsilon_2) \quad , \tag{69}$$

and we calculate that

$$E_{\text{rms}}^2 = \tfrac{70}{9}\Gamma_0^2[1 + (9\epsilon_2^2/125\Gamma_0^2) + (18\epsilon_0^2/175\Gamma_0^2)] \, . \tag{70}$$

These two quantities are quite insensitive to values of ϵ_0 and ϵ_2 of less than, say, 0.25. For example, with

$$(\epsilon_0/\Gamma_0) = (\epsilon_2/\Gamma_0) = 0.20 \quad ,$$

the values of E_{rms}^2 and ΔE are changed by less than 2% from the values they would have in the presence of EQQ interactions only. Thus, using the criterion that E_{rms}^2 and ΔE should not be noticeably affected by the inclusion of non-EQQ interactions (since the experimental results mentioned above are adequately explained without employing such interactions) does not allow us to make a very definite prediction of the magnitude of (ϵ_0/Γ_0) and (ϵ_2/Γ_0), except to state that (ϵ_0/Γ_0) and (ϵ_2/Γ_0) are less than, say, 0.25.

One might imagine, then, that these parameters would have no significant effect on the libron spectrum. This however, is not the case, as can be seen from Tables II and III. Taking $\epsilon_0 = \epsilon_2 = 0$ for the C_{mmm} structure we obtain a very poor fit to the data, as is apparent from Figs. 2 and 3. If one admits nonzero values of these parameters, then it is possible to obtain an exact fit to the frequencies. The resulting values of ϵ_0 and ϵ_2 are unreasonably large, however. If ϵ_0 and ϵ_2 are restricted to be at most 0.20 cm^{-1} in magnitude, then even the "best" fit (see Figs. 2 and 3) is unacceptable. Since assuming the C_{mmm} structure involves not only taking anomalously large values of ϵ_0 and ϵ_2, but also fails to give an adequate fit to the observed Raman intensities, we feel that this structure is quite unlikely. This conclusion is in agreement with the neutron-diffraction data of Mucker *et al.*[11]

Let us therefore confine our attention to the $Pa3$ structure. As can be seen from Figs. 4 and 5, a qualitative fit to the experimental data can be obtained even in the absence of non-EQQ interactions. It is seen, however, that the calculated frequencies in this case do not agree perfectly with experiment, the discrepancy being particu-

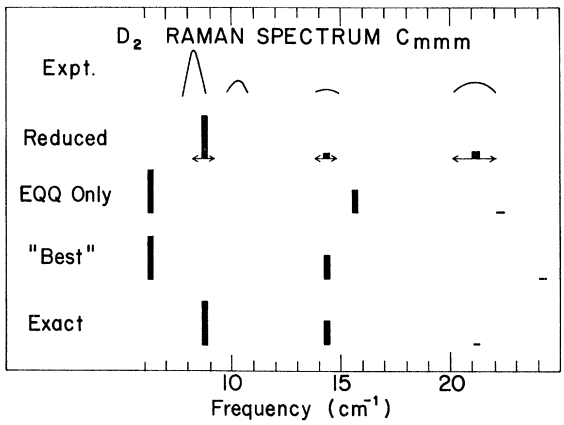

FIG. 3. Fit to the Raman data of Ref. 7 for solid D_2 assuming the C_{mmm} structure. For an explanation see the caption of Fig. 2. Here the parameters are EQQ only: $\Gamma_{\text{expt}} = 0.78$; "best" fit: $\Gamma_{\text{expt}} = 0.85$, $\epsilon_2 = -0.20$, $\epsilon_0 = -0.20$; exact fit: $\Gamma_{\text{expt}} = 0.66$, $\epsilon_2 = 0.87$, $\epsilon_0 = -0.28$.

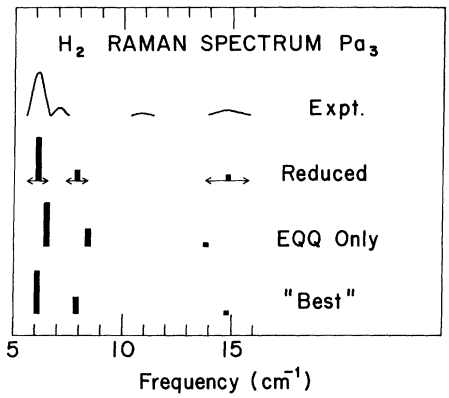

FIG. 4. Fit to the Raman data of Ref. 7 for solid H_2 assuming the $Pa3$ structure. For an explanation see the caption of Fig. 2. Here the parameters are EQQ only: $\Gamma_{expt} = 0.475$; exact fit: $\Gamma_{expt} = 0.516$, $\epsilon_2 = 0.14$, $\epsilon_0 = 0.06$.

larly noticeable for D_2. By permitting small nonzero values of ϵ_0 and ϵ_2, we can reproduce the "reduced" experimental spectrum exactly, as is seen from Figs. 4 and 5.

Note that we have treated Γ_0 as an adjustable parameter, which we denote Γ_{expt}, since there may be some uncertainties in the calculation of the renormalization coefficient ξ_0 introduced in Eq. (3). According to the renormalization calculations cited in Table I, we expect that

$$\Gamma_{expt} = \xi_{rot}\,\xi_0\,\Gamma_0 \equiv \xi\,\Gamma_0 \quad . \tag{71}$$

However, since the libron-libron interactions are so strong, it is very important to consider their effect on each mode separately, rather than in the average way implied by the introduction of ξ_{rot} in Eq. (68b). In view of this uncertainty, we do not feel that a meaningful determination of ϵ_0 or ϵ_2 is possible at present. Since these parameters do influence the libron spectrum, it would be of interest to plot out the libron spectrum via inelastic scattering of neutrons. In this way it should be possible to determine all the interactions accurately. As for the magnitude of ξ, from Figs. 4 and 5 we see that $\Gamma_{expt} = 0.48\ cm^{-1}$ for H_2 and $\Gamma_{expt} = 0.64\ cm^{-1}$ for D_2, so that experimentally, we have

$$\xi = 0.69 \quad \text{for } H_2 \ , \tag{72a}$$

$$\xi = 0.76 \quad \text{for } D_2 \ . \tag{72b}$$

Considering the discrepancy between the theoretical estimates for ξ in Table I and these experimental values, further investigation of these effects is indicated.

B. Summary

We may summarize our work as follows: (i) The $Pa3$ structure is a reasonable first approximation and an adequate fit to the Raman spectrum can be obtained assuming only EQQ interactions. (ii) The C_{mmm} structure is quite unlikely, as neither the intensities nor the frequencies of the Raman spectrum agree very well with experiment. (iii) The determination of the magnitudes of the non-EQQ interactions is not possible through the thermodynamic measurements mentioned, and hence such measurements do not establish the smallness of these interactions. On the other hand, the libron spectrum is much more sensitive to these interactions. (iv) The effect of libron-libron interactions on the frequencies of the elementary excitations has been calculated in an approximate way and energy shifts of order 15% have been found. (v) When the above-mentioned libron-libron interactions are taken into account, it is found that current theoretical estimates of the renormalized EQQ interaction coefficient $\xi\Gamma$ differs by about 10% from the experimental values.

Based on our work, we may indicate several fruitful lines of investigation. First, since the determination of the structure of solid hydrogen is not yet complete, we suggest that further study of the libron spectrum using inelastic scattering of neutrons would be desirable. This type of experiment would also enable a reasonable determination of all the interactions between hydrogen molecules. Second, a better calculation of the many-body effects on the EQQ

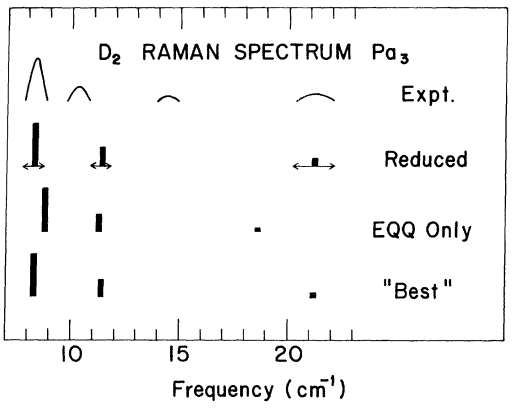

FIG. 5. Fit to the Raman data of Ref. 7 for solid D_2 assuming the $Pa3$ structure. For an explanation see the caption of Fig. 2. Here the parameters are EQQ only: $\Gamma_{expt} = 0.640$; exact fit: $\Gamma_{expt} = 0.744$, $\epsilon_2 = 0.16$, $\epsilon_0 = -0.13$.

interactions is needed, in order to make the interpretation of the experiments more secure. Along this line, it is important to study dynamical libron-phonon interactions. Finally, we are presently undertaking a detailed calculation of libron-libron interactions so as to be able to predict the energy shift and energy width of all the zero-wave-vector modes due to these interactions.

ACKNOWLEDGMENTS

We would like to thank A. J. Berlinsky for his assistance in some of the numerical calculations. We also profited from several discussions with Professor H. Meyer. We would like to thank Professor H. James for discussing some of his results prior to publication.

APPENDIX A: LIBRATIONAL EXCITATIONS IN CLASSICAL SYSTEMS

In this Appendix, we shall consider the librational excitations of a classical system with EQQ interactions between molecules. From Eq. (5), we obtain the potential energy of such a system in the form

$$\mathcal{H} = \sum_{ij} \sum_{mm'} \gamma_{ij}^{mm'} O_i^m O_j^{m'} \ , \tag{A1}$$

where the $\gamma_{ij}^{mm'}$ are defined in Eq. (9). We wish to consider the small oscillations of the molecules about their equilibrium orientations. For this purpose it is convenient to introduce the direction cosines (x_i, y_i, z_i) of the molecular axis of the ith molecule and expand the potential energy to second order in the direction cosines x_i and y_i. In terms of the direction cosines the spherical harmonics in Eq. (A1) may be written

$$O_i^{\pm 2} = -\tfrac{5}{2}(x_i \pm iy_i)^2 \ , \tag{A2a}$$

$$O_i^{\pm 1} = -5 z_i (x_i \pm iy_i) \ , \tag{A2b}$$

$$O_i^0 = -\tfrac{5}{2}(3z_i^2 - 1) \ . \tag{A2c}$$

Note that the direction cosines are not all independent, but must satisfy

$$x_i^2 + y_i^2 + z_i^2 = 1 \ . \tag{A3}$$

We may use this relation to eliminate z_i in favor of x_i and y_i. In particular, when x_i and y_i are small, we have

$$z_i = 1 - \tfrac{1}{2}x_i^2 - \tfrac{1}{2}y_i^2 \ . \tag{A4}$$

By taking advantage in this way of the assumption of small oscillations we obtain a much simpler formulation than that of Ref. 18.

On expanding the potential energy in powers of the direction cosines x_i and y_i and making use of Eq. (A4), the quadratic terms, denoted V, are found to be

$$\begin{aligned} \tfrac{4}{25} V = a \sum_i (x_i^2 + y_i^2) + 4 \sum_{ij} [& \gamma_{ij}^{11} (x_i + iy_i)(x_j + iy_j) \\ & + (\gamma_{ij}^{11})^* (x_i - iy_i)(x_j - iy_j) + \gamma_{ij}^{1,-1} (x_i + iy_i)(x_j - iy_j) \\ & + (\gamma_{ij}^{1,-1})^* (x_i - iy_i)(x_j + iy_j) \\ & + \gamma_{ij}^{20} (x_i + iy_i)^2 + (\gamma_{ij}^{20})^* (x_i - iy_i)^2] \ , \end{aligned} \tag{A5}$$

in close analogy to Eq. (18) for the quantum system. The expression for the kinetic energy may be written

$$T = \tfrac{1}{2} I \sum_i (\dot{x}_i^2 + \dot{y}_i^2) \ , \tag{A6}$$

where I is the moment of inertia of the molecules, and we have used Eq. (A4) to drop the terms in $\dot{z}_i$.

From these expressions for the kinetic and potential energies, the equations of motion for the direction cosines are found to be

$$\begin{aligned} \tfrac{4}{25} I(\ddot{x}_i + i\ddot{y}_i) = & -a(x_i + iy_i) + b(x_i - iy_i) \\ & - 8 \sum_j [(\gamma_{ij}^{11})^* (x_j - iy_j) + (\gamma_{ij}^{1,-1})^* (x_j + iy_j)] \ , \end{aligned} \tag{A7a}$$

$$\begin{aligned} \tfrac{4}{25} I(\ddot{x}_i - i\ddot{y}_i) = & -a(x_i - iy_i) + b(x_i + iy_i) \\ & - 8 \sum_j [\gamma_{ij}^{11} (x_j + iy_j) + \gamma_{ij}^{1,-1} (x_j - iy_j)] \ , \end{aligned} \tag{A7b}$$

where a and b are as defined in Eq. (18). As in the quantum treatment it is convenient to introduce spatial Fourier transforms by defining

$$x_\alpha(\vec{k}) = (s/N)^{1/2} \sum_{j(\alpha)} x_{j(\alpha)} \exp[-i\vec{k} \cdot \vec{R}_{j(\alpha)}] \ , \tag{A8a}$$

$$y_\alpha(\vec{k}) = (s/N)^{1/2} \sum_{j(\alpha)} y_{j(\alpha)} \exp[-i\vec{k} \cdot \vec{R}_{j(\alpha)}] \ . \tag{A8b}$$

Assuming harmonic time dependence, we may rewrite the equations of motion as

$$\begin{aligned} & \tfrac{4}{25} I \omega^2 [x_\alpha(\vec{k}) + iy_\alpha(\vec{k})] \\ & = a[x_\alpha(\vec{k}) + iy_\alpha(\vec{k})] - b[x_\alpha(\vec{k}) - iy_\alpha(\vec{k})] \\ & \quad + 8 \sum_\beta \gamma_{\alpha\beta}^{11}(\vec{k})^* [x_\beta(\vec{k}) - iy_\beta(\vec{k})] \\ & \quad + 8 \sum_\beta \gamma_{\alpha\beta}^{1,-1}(\vec{k})^* [x_\beta(\vec{k}) + iy_\beta(\vec{k})] \ , \end{aligned} \tag{A9a}$$

$$\tfrac{4}{25} I \omega^2 [x_\alpha(\vec{k}) - iy_\alpha(\vec{k})]$$

$$= a[x_\alpha(\vec{k}) - iy_\alpha(\vec{k})] - b[x_\alpha(\vec{k}) + iy_\alpha(\vec{k})]$$
$$+ 8\sum_\beta \gamma^{11}_{\alpha\beta}(\vec{k})[x_\beta(\vec{k}) + iy_\beta(\vec{k})]$$
$$+ 8\sum_\beta \gamma^{1,-1}_{\alpha\beta}(\vec{k})[x_\beta(\vec{k}) - iy_\beta(\vec{k})] \,. \qquad \text{(A9b)}$$

In terms of vector notation, these equations are

$$\tfrac{4}{25} I\omega^2 \begin{pmatrix} \psi^+(\vec{k}) \\ \psi^-(\vec{k}) \end{pmatrix} = [a\underline{I} + b\underline{\sigma} + 2\underline{F}(\vec{k})] \begin{pmatrix} \psi^+(\vec{k}) \\ \psi^-(\vec{k}) \end{pmatrix}, \qquad \text{(A10)}$$

where the matrices $\underline{I}$, $\underline{\sigma}$, and $\underline{F}(\vec{k})$ are defined in Eq. (20), and the subvectors $\psi^+(\vec{k})$ and $\psi^-(\vec{k})$ are s-dimensional vectors with components

$$\psi^\pm_\alpha(\vec{k}) = [\pm x_\alpha(\vec{k}) - iy_\alpha(\vec{k})], \quad \alpha = 1, 2, \cdots, s \,.$$

For the $Pa3$ structure we have $b = 0$, and it is easily seen that the eigenfrequencies ω_Q for the quantum system, given by Eq. (28) in the main body of this paper, are proportional to those of the classical system, ω_{cl}, given in Eq. (A10). This scaling relation holds throughout the Brillouin zone. For the C_{mmm} structure no such simple relation obtains, because for this structure b is nonzero. Even for the $Pa3$ structure note that the correspondence is not the usual one between the classical and quantum treatments of the harmonic oscillator. In the usual correspondence, the frequencies are identical, only the amplitudes differ, since they are quantized in the quantum limit. As mentioned in the text, the correct exact correspondence is between the classical system and the quantum systems for which B is much less than a typical libron energy.

APPENDIX B: TABULATION OF γ^{mn}_{ij} FOR $Pa3$ STRUCTURE

In this Appendix, we shall discuss the evaluation and tabulation of the interaction coefficients γ^{mn}_{ij} for the $Pa3$ structure. For this purpose, we shall enumerate several properties of these coefficients, omitting proofs for economy of presentation.

The $Pa3$ structure is formed from a simple-cubic Bravais lattice with a basis specified by the four sublattice vectors $\vec{\tau}_\alpha$ given in Table VI, so that each unit cell contains four molecules. The position of the ith molecule $\vec{R}_i$ is given by

$$\vec{R}_i = \vec{R} + \vec{\tau}_\alpha \,, \qquad \text{(B1a)}$$

with $\vec{R}$ being a translation vector of the Bravais lattice,

$$\vec{R} = l\vec{a}_1 + m\vec{a}_2 + n\vec{a}_3 \,, \qquad \text{(B1b)}$$

where $\vec{a}_1$, $\vec{a}_2$, $\vec{a}_3$ are the primitive translation vectors of the Bravais lattice and l, m, n are integers. The choice of $\vec{a}_1$, $\vec{a}_2$, $\vec{a}_3$ is not unique and they will be taken here as $\vec{a}_1 = a\hat{i}$, $\vec{a}_2 = a\hat{j}$, and $\vec{a}_3 = a\hat{k}$, where a is the length of the cube edge and $\hat{i}$, $\hat{j}$, $\hat{k}$ are the unit vectors along the crystal axes.

From the discussion above we see that to specify the position of each molecule requires two labels: one labeling the unit cell $\vec{R}$ and one labeling the sublattice within that unit cell $\vec{\tau}_\alpha$. In order to display the relationship among the coefficients γ^{mn}_{ij} we define (within this Appendix only)

$$\gamma^{mn}_{ij} \equiv \gamma^{mn}_{\alpha\beta}(\vec{R}, \vec{R}') \equiv \gamma^{mn}_{\alpha\beta}(\vec{R}' - \vec{R}) \,, \qquad \text{(B2)}$$

with $\vec{R}_i = \vec{R} + \vec{\tau}_\alpha$ and $\vec{R}_j = \vec{R}' + \vec{\tau}_\beta$. The notation is taken to indicate that the interaction coefficients γ^{mn}_{ij} are calculated between the jth molecule which is on sublattice β in the $\vec{R}'$th unit cell and the ith molecule which is on sublattice α in the $\vec{R}$th unit cell and $\vec{R}' - \vec{R}$ is the translation vector between the unit cells.

Working in the "crystal" coordinate system of Eq. (B1b) one can show that

$$(-1)^m \gamma^{-m,n}_{42}(\sigma_{\hat{k}}\vec{R}) = (-1)^m \gamma^{n,-m}_{24}(-\sigma_{\hat{k}}\vec{R})$$
$$= \gamma^{nm}_{31}(-\vec{R}) = \gamma^{mn}_{13}(\vec{R}) \,, \qquad \text{(B3a)}$$

$$(-1)^m \gamma^{n,-m}_{32}(\sigma_{\hat{j}}\vec{R} + a\hat{k})^* = (-1)^m \gamma^{-m,n}_{23}(-a\hat{k} - \sigma_{\hat{j}}\vec{R})^*$$
$$= \gamma^{mn}_{41}(-\vec{R}) = \gamma^{nm}_{14}(\vec{R}) \,, \qquad \text{(B3b)}$$

$$(-1)^n \gamma^{m,-n}_{34}(\sigma_{\hat{j}}\vec{R})^* = (-1)^n \gamma^{-n,m}_{43}(-\sigma_{\hat{j}}\vec{R})^*$$
$$= \gamma^{nm}_{21}(-\vec{R}) = \gamma^{mn}_{12}(\vec{R}) \,, \qquad \text{(B3c)}$$

where the operator $\sigma_{\hat{n}}$ is defined as a reflection in a plane perpendicular to $\hat{n}$:

$$\sigma_{\hat{n}}\vec{R} \equiv \vec{R} - 2\hat{n}(\hat{n} \cdot \vec{R}) \,. \qquad \text{(B4)}$$

Taking the quantization axis along the local symmetry axis, one obtains directly the evaluation

TABLE VI. Position and equilibrium orientation of sites.

β[a]	Sublattice[b]	Direction of z axis	Direction of x axis
1	$\frac{1}{2}a(0, 0, 0)$	[1, 1, 1]	[1, 1, −2]
2	$\frac{1}{2}a(1, 1, 0)$	[−1, 1, 1]	[−1, 1, −2]
3	$\frac{1}{2}a(0, 1, 1)$	[1, −1, 1]	[1, −1, −2]
4	$\frac{1}{2}a(1, 0, 1)$	[1, 1, −1]	[−1, −1, −2]

[a]Here β labels the sublattice

[b]Here $a = \sqrt{2}\,R_0$, where R_0 is the nearest-neighbor separation.

$$\gamma_{11}^{mn}(\vec{R}) = 4\pi A_m A_n \sum_J \epsilon_J(R)\,\alpha_J\,[\pi/(2J+1)]^{1/2} \times C(22J; m, n)\, Y_J^{m+n}(\hat{R})_1 \ , \qquad \text{(B5)}$$

where the subscript 1 indicates that the coordinate system coincides with the symmetry axes of site 1. Similar relations hold when the script 1 is replaced by 2, 3, or 4, and the $\gamma_{\alpha\alpha}^{mn}(\vec{R})$ can be related to $\gamma_{11}^{mn}(\vec{R})$. It is clear from these relations that it suffices to tabulate $\gamma_{1\alpha}^{mn}(\vec{R})$.

By using the symmetry associated with the threefold axis along the [111] directions, the number of independent coefficients can be reduced still further. We find that

$$(-1)^n \gamma_{14}^{mn}([\mathcal{R}']^2 \vec{R}) \exp[\tfrac{4}{3}\pi i(m-n)] = \gamma_{13}^{mn}(\mathcal{R}'\vec{R}) \exp[\tfrac{2}{3}\pi i(m-n)] = \gamma_{12}^{mn}(\vec{R}) \ , \qquad \text{(B6)}$$

where

$$\mathcal{R}'(A\hat{i} + B\hat{j} + C\hat{k}) \equiv C\hat{i} + A\hat{j} + B\hat{k} \qquad \text{(B7)}$$

is a rotation about the crystal [111] direction. Thus it is only necessary to tabulate $\gamma_{11}^{mn}(\vec{R})$ and $\gamma_{12}^{mn}(\vec{R})$, In fact, in this tabulation $\vec{R}$ can be limited to the first quadrant, $R_x \geq 0$, $R_z \geq 0$, in view of the relations

$$\gamma_{ij}^{mn} = \gamma_{ik}^{mn} \quad \text{if } \vec{R}_{ij} = -\vec{R}_{ik} \ , \qquad \text{(B8a)}$$

$$\gamma_{12}^{mn}(\vec{R})^* = \gamma_{12}^{nm}(\sigma_i \vec{R} - a\hat{i}) \ . \qquad \text{(B8b)}$$

We shall tabulate the $\gamma_{\alpha\beta}^{mn}(\vec{R})$ for EQQ interactions only between nearest neighbors. Then $\gamma_{11}^{mn}(\vec{R}) = 0$ and $\gamma_{12}^{mn}(\vec{R})$ is given in Table VII. From this tabulation, all nonvanishing γ_{ij}^{mn} can be determined by the following procedure: (a) Complete the tabulation of $\gamma_{12}^{mn}(0)$ by using $\gamma_{12}^{-m,-n}(0) = [\gamma_{12}^{mn}(0)]^*$. (b) Evaluate the other nonvanishing $\gamma_{12}^{mn}(\vec{R})$ for nearest-neighbor interactions, i.e., for $\vec{R} = a(-1,0,0)$, $\vec{R} = a(0,-1,0)$, and $\vec{R} = a(-1,-1,0)$ from Eqs. (B8a) and (B8b). (c) Compute $\gamma_{1\beta}^{mn}$ by using Eq. (B6). (d) Complete the tabulation of $\gamma_{\alpha\beta}^{mn}$ by using Eq. (B3). We have verified that the tabulated values satisfy the sum rule

$$\sum_{mn} |\gamma_{12}^{mn}(0)/A_m A_n|^2 = \tfrac{1750}{9}\pi^2 \Gamma_0^2 \ , \qquad \text{(B9)}$$

which can be derived using the orthogonality relations of the spherical harmonics and rotation matrices.

The values of γ_{ij}^{mn} can also be used to calculate the moments of the frequency distribution I_n which are defined as

$$I_n = (8N)^{-1} \sum_{\vec{k},\mu} [\hbar\omega_\mu(\vec{k})/a]^n \ . \qquad \text{(B10)}$$

From Eq. (28), we see that for the $Pa3$ structure (where $b = 0$)

$$\sum_{\vec{k},\mu} [\hbar\omega_\mu(\vec{k})/a]^n = \mathrm{Tr}[\underline{I} + 2a^{-1}\underline{F}(\vec{k})]^{n/2} \qquad \text{(B11a)}$$

$$= \mathrm{Tr}[\underline{I} + na^{-1}\underline{F}(\vec{k}) + \cdots] \ , \qquad \text{(B11b)}$$

so that I_n can be evaluated in terms of traces of powers of $\underline{F}(\vec{k})$, or equivalently, as sums over γ_{ij}^{mn}. Since these sums are again series in the parameter $1/z$, we truncate them at the lowest nontrival order:

$$(8N)^{-1} \sum_{\vec{k},\mu} \left(\frac{\hbar\omega_\mu(\vec{k})}{a}\right)^n = 1 + \frac{n(n-2)}{16N} \sum_{\vec{k}} \mathrm{Tr}\left(\frac{F(\vec{k})}{a}\right)^2 \ . \qquad \text{(B12)}$$

For nearest-neighbor EQQ interactions only, $a = 19\Gamma_0$, and we may use the values of Table VII for γ_{ij}^{mn}. Then we find the numerical results

$$I_{+2} = 1.0000\,(1.0000) \ , \qquad \text{(B13a)}$$

$$I_{+1} = 0.9835\,(0.9832) \ , \qquad \text{(B13b)}$$

$$I_0 = 1.0000\,(1.0000) \ , \qquad \text{(B13c)}$$

TABLE VII. Values[a] of $\gamma_{12}^{mn}(0)$ for the $Pa3$ structure with nearest-neighbor EQQ interactions.

m/n	2	1	0
2	(−0.6737, −0.4811)[b]	(−0.6678, 0.2041)[b]	(−0.3194, 0.1925)[b]
1	(−1.5517, −0.2040)	(−0.5556, 0.2405)	(−0.6678, −0.1361)
0	(−0.7360, 0.7697)	(−0.0786, −0.5443)	(−0.5277, −0.0000)
−1	(−0.6088, −0.3401)	(0.7777, 0.1443)	(−0.6678, 0.1361)
−2	(−0.0070, −0.2886)	(0.2750, 0.3402)	(−0.3194, −0.1925)

[a]We tabulate values of $4\gamma_{12}^{mn}(0)/\Gamma_0$. For $n < 0$, it is necessary to use the relation $\gamma_{12}^{mn}(0)^* = \gamma_{12}^{-m,-n}(0)$.

[b]Here (x, y) denotes $x + iy$.

$$I_{-1} = 1.0494\,(1.0543)\ , \tag{B13d}$$

$$I_{-2} = 1.1318\,(1.1541)\ . \tag{B13e}$$

For comparison we have also included in parenthesis Raich and Etter's corrected values.[43] Note that our results, correct to lowest nontrivial order in $1/z$ are in excellent agreement with their values which were obtained by performing sums over the Brillouin zone. It is also quite clear that the effects of further neighbors are negligible in low-order perturbation theory. This is because the summands in Eqs. (61), (62), (67), and (B12) vary with separation as (R_0/R).[10]

---

*Work supported in part by the Office of Naval Research, National Science Foundation, and the Advanced Research Projects Agency.

[1]By hydrogen we mean any of the hydrogenic isotopes. Specific isotopic moleclues are denoted H_2, HD, etc.

[2]S. Homma, K. Okada, and H. Matsuda, Progr. Theoret. Phys. (Kyoto) 36, 1310 (1966); 38, 767 (1967).

[3]H. Ueyama and T. Matsubara, Progr. Theoret. Phys. (Kyoto) 36, 784 (1967).

[4]J. C. Raich and R. D. Etters, Phys. Rev. 168, 425 (1968).

[5]F. G. Mertens, W. Biem, and H. Hahn, Z. Physik 213, 33 (1968).

[6]A. J. Berlinsky, A. B. Harris, and C. F. Coll, III, Solid State Commun. 7, 1491 (1969).

[7]W. N. Hardy, I. F. Silvera, and J. P. McTague, Phys. Rev. Letters 22, 297 (1969).

[8]By a distortion we mean either a distortion in the center of gravity of the molecules or a distortion in their orientations. This distortion may or may not increase the size of the "magnetic" unit cell.

[9]H. M. James, Lecture at the International Conference on Quantum Crystals, Aspen, 1969 (unpublished).

[10]W. N. Hardy, Lecture at the International Conference on Quantum Crystals, Aspen, 1969 (unpublished).

[11]K. F. Mucker, P. M. Harris, D. White, and R. A. Erickson, J. Chem. Phys. 49, 1922 (1968).

[12]H. M. James, Phys. Rev. Letters 24, 815 (1970); and to be published .

[13]I. F. Silvera (private communication).

[14]T. Oguchi, Phys. Rev. 117, 117 (1960).

[15]A. B. Harris, Phys. Rev. Letters 21, 602 (1968).

[16]T. Nakamura (unpublished).

[17]O. Schnepp, J. Chem. Phys. 46, 3983 (1967).

[18]S. H. Walmsley and J. A. Pople, Mol. Phys. 8, 345 (1964).

[19]This scaling relation was noted in Ref. 7.

[20]T. Nakamura, Progr. Theoret. Phys. (Kyoto) 14, 135 (1955).

[21]M. E. Rose, *Elementary Theory of Angular Momentum* (Wiley, New York, 1957). We use Rose's phase convention for the spherical harmonics, rotation matrices, and Clebsch-Gordan coefficients, and also his notation for the Euler angles.

[22]J. Van Kranendonk, Can. J. Phys. 25, 1080 (1959).

[23]H. Margenau, Phys. Rev. 64, 131 (1943).

[24]J. deBoer, Physica 9, 363 (1942).

[25]A. B. Harris, Intern. J. Quantum Chem. 2S, 347 (1968); in *Proceedings of the Eleventh International Conference on Low-Temperature Physics*, edited by J. F. Allen, D. M. Finlayson, and D. M. McCall (University of St. Andrews Printing Department, St. Andrews, Scotland, 1969), Vol. I, p. 608; Phys. Rev. B 1, 1881 (1970).

[26]J. Noolandi and J. Van Kranendonk, Phys. Letters 30A, 258 (1969).

[27]The C_{mmm} structure is cubic with successive xy planes having all molecules oriented along the x axis and y axis, alternately. For the $Pa3$ structure the ground state is described in J. Felsteiner, Phys. Rev. Letters 15, 200 (1965). The exact placement and orientation of the sublattices is specified in Table VI in Appendix B. [*Note added in proof.* The designation C_{mmm} appears to be incorrect. The point group of the structure proposed in Ref. 12 for which we have calculated the libron spectrum is D_{4h}. The correct space group is $P4_2/mnm\ (D_{4h}^{14})$. Needless to say, the confusion in nomenclature does not affect the numerical results of Ref. 12 or this work.]

[28]L. I. Amstutz, H. Meyer, S. M. Myers, and D. C. Rorer, Phys. Rev. 181, 589 (1969).

[29]D. Ramm, H. Meyer, J. F. Jarvis, and R. L. Mills, Solid State Commun. 6, 497 (1968); D. Ramm, H. Meyer, and R. L. Mills, Phys. Rev. B 1, 2763 (1970).

[30]F. J. Dyson, Phys. Rev. 102, 1217 (1956); 102, 1230 (1956).

[31]R. Silberglitt and A. B. Harris, Phys. Rev. Letters 19, 30 (1967); Phys. Rev. 174, 640 (1968).

[32]A. B. Harris, D. Kumar, B. I. Halperin, and P. C. Hohenberg, J. Appl. Phys. 41, 1361 (1970).

[33]T. Holstein and H. Primakoff, Phys. Rev. 58, 1098 (1940).

[34]S. V. Maleev, Zh. Eksperim. i Teor. Fiz. 33, 1010 (1957) [Soviet Phys. JETP 6, 776 (1958)].

[35]L. I. Schiff, *Quantum Mechanics* (McGraw-Hill, New York, 1955), Chap. XIV.

[36]The Raman scattering amplitude depends on the kinetic energy of the scattered photon via the density of final states. Thus our calculation is only valid when, as is usual, the photon energies are much larger than the libron energy.

[37]C. Bloch and C. deDominicis, Nucl. Phys. 7, 459 (1958); R. Balian and C. deDominicis, Compt. Rend. 250, 3285 (1960).

[38]A. B. Harris, J. Phys. Chem. Solids 27, 1927 (1966).

[39]G. Grenier and D. White, J. Chem. Phys. 40, 3015 (1964).

[40]A. J. Berlinsky and A. B. Harris, Phys. Rev. A 1, 878 (1970).

[41]J. F. Jarvis, H. Meyer, and D. Ramm, Phys. Rev. 178, 1461 (1969).

[42]A. B. Harris, L. I. Amstutz, H. Meyer, and S. M. Myers, Phys. Rev. 175, 603 (1968).

[43]J. C. Raich (private communication).